

INTRODUCTION

As a pervasive disturbance agent operating at many spatial and temporal scales, wildland fire is a key abiotic factor affecting forest health both positively and negatively. In some ecosystems, for example, wildland fires have been essential for regulating processes that maintain forest health (Lundquist and others 2011). Wildland fire is an important ecological mechanism that shapes the distributions of species, maintains the structure and function of fire-prone communities, and acts as a significant evolutionary force (Bond and Keeley 2005). At the same time, wildland fires have created forest health (i.e., sustainability) problems in some ecosystems (Edmonds and others 2011). Specifically, fire outside the historic range of frequency and intensity can impose extensive ecological and socioeconomic impacts. Current fire regimes on more than half of the forested area in the conterminous United States have been moderately or significantly altered from historical regimes, potentially altering key ecosystem components such as species composition, structural stage, stand age, canopy closure, and fuel loadings (Schmidt and others 2002). As a result of intensive fire suppression efforts during most of the 20th century, the forest area burned annually decreased from approximately 16–20 million ha (40–50 million acres) in the early 1930s to about 2 million ha

(5 million acres) in the 1970s (Vinton 2004). Understanding existing fire regimes is essential for properly assessing the impact of fire on forest health because changes to historical fire regimes can alter forest developmental patterns, including the establishment, growth, and mortality of trees (Lundquist and others 2011).

Fire regimes have been dramatically altered by fire suppression (Barbour and others 1999) and by the introduction of nonnative invasive plants, which can change fuel properties and in turn both affect fire behavior and alter fire regime characteristics such as frequency, intensity, type, and seasonality (Brooks and others 2004). Fires in some regions and ecosystems have become larger, more intense, and more damaging because of the accumulation of fuels as a result of prolonged fire suppression (Pyne 2010). Such large wildland fires also can have long-lasting social and economic consequences, which include the loss of human life and property, smoke-related human health impacts, and the economic cost and dangers of fighting the fires themselves (Gill and others 2013, Richardson and others 2012). In some regions, plant communities have experienced or are undergoing rapid compositional and structural changes as a result of fire suppression (Nowacki and Abrams 2008). Additionally, changes in fire intensity and recurrence could result in decreased forest resilience and persistence

CHAPTER 3.

Large-Scale Patterns of Forest Fire Occurrence across the 50 United States and the Caribbean Territories, 2017

KEVIN M. POTTER

(Lundquist and others 2011), and fire regimes altered by global climate change could cause large-scale shifts in vegetation spatial patterns (McKenzie and others 1996). Given the relationships of fires to forest dynamics, it is important to monitor and assess spatiotemporal trends in forest fires across the United States and its territories.

This chapter presents analyses of daily satellite-based fire occurrence data that map and quantify the locations and intensities of fire occurrences spatially across the conterminous United States, Alaska, Hawaii, and the Caribbean territories in 2017. It also compares 2017 fire occurrences, within a geographic context, to all the recent years for which such data are available. Quantifying and monitoring such large-scale patterns of fire occurrence across the United States can help improve our understanding of the ecological and economic impacts of fire as well as the appropriate management and prescribed use of fire. Specifically, large-scale assessments of fire occurrence can help identify areas where specific management activities may be needed, or where research into the ecological and socioeconomic impacts of fires may be required.

METHODS

Data

Annual monitoring and reporting of active wildland fire events using the Moderate Resolution Imaging Spectroradiometer (MODIS)

Active Fire Detections for the United States database (USDA Forest Service 2018) allow analysts to spatially display and summarize fire occurrences across broad geographic regions (Coulston and others 2005; Potter 2012a, 2012b, 2013a, 2013b, 2014, 2015a, 2015b, 2016, 2017, 2018). A fire occurrence is defined as one daily satellite detection of wildland fire in a 1-km pixel, with multiple fire occurrences possible on a pixel across multiple days resulting from a single wildland fire that lasts more than a single day. The data are derived using the MODIS Rapid Response System (Justice and others 2002, 2011) to extract fire location and intensity information from the thermal infrared bands of imagery collected daily by two satellites at a resolution of 1 km, with the center of a pixel recorded as a fire occurrence (USDA Forest Service 2018). The Terra and Aqua satellites' MODIS sensors identify the presence of a fire at the time of image collection, with Terra observations collected in the morning and Aqua observations collected in the afternoon. The resulting fire occurrence data represent only whether a fire was active because the MODIS data bands may not differentiate between a hot fire in a relatively small area (0.01 km², for example) and a cooler fire over a larger area (1 km², for example) if the foreground to background temperature contrast is not sufficiently high. The MODIS Active Fire database does well at capturing large fires during cloud-free conditions but may underrepresent rapidly burning, small, and low-intensity fires,

as well as fires in areas with frequent cloud cover (Hawbaker and others 2008). For large-scale assessments, the dataset represents a good alternative to the use of information on ignition points, which may be preferable but can be difficult to obtain or may not exist (Tonini and others 2009). For more information about the performance of this product, see Justice and others (2011).

It is important to underscore that estimates of burned area and calculations of MODIS-detected fire occurrences are two different metrics for quantifying fire activity within a given year. Most importantly, the MODIS data contain both spatial and temporal components because persistent fire will be detected repeatedly over several days on a given 1-km pixel. In other words, a location can be counted as having a fire occurrence multiple times, once for each day a fire is detected at the location. Analyses of the MODIS-detected fire occurrences, therefore, measure the total number of daily 1-km pixels with fire during a year, as opposed to quantifying only the area on which fire occurred at some point during the course of the year. A fire detected on a single pixel on every day of the year would be equivalent to 365 fire occurrences.

It is worth noting that the Terra and Aqua satellites, which carry the MODIS sensors, were launched in 1999 and 2002, respectively,

and will eventually be decommissioned. An alternative fire occurrence data source is the Visible Infrared Imaging Radiometer Suite (VIIRS) sensor on board the Suomi National Polar-orbiting Partnership (Suomi NPP) weather satellite. The transition to this new data source will require a comparison of fire occurrence detections between it and MODIS.

Analyses

These MODIS products for 2017, and for the 16 preceding full years of data, were processed in ArcMap[®] (ESRI 2015) to determine the number of fire occurrences per 100 km² (10 000 ha) of forested area for each ecoregion section in the conterminous United States (Cleland and others 2007) and Alaska (Nowacki and Brock 1995), and for each of the major islands of Hawaii and of the Caribbean territories of Puerto Rico and the U.S. Virgin Islands. This forest fire occurrence density measure for the conterminous 48 States and Alaska was calculated after screening out wildland fires on nonforested pixels using a forest cover layer derived from MODIS imagery by the U.S. Department of Agriculture Forest Service, Remote Sensing Applications Center (RSAC) (USDA Forest Service 2008). The same process was repeated for the Hawaiian islands using 30-m vegetation type data from the LANDFIRE program (LANDFIRE 2014), resampled to 1 km, and for Puerto Rico and the U.S. Virgin Islands

using 30-m landcover data (also resampled to 1 km) from the Forest Service International Institute of Tropical Forestry (IITF) that were derived from a cloud-free Landsat image mosaic developed in cooperation with RSAC (Kennaway and Helmer 2007, Kennaway and others 2008). The total numbers of forest fire occurrences were also determined separately for the conterminous States, Alaska, Hawaii, and the Caribbean territories.

The fire occurrence density value for each of the ecoregion sections and the Hawaiian and Caribbean islands in 2017 was then compared with the mean fire density values for the first 16 full years of MODIS Active Fire data collection (2001–2016). Specifically, the difference of the 2017 value and the previous 16-year mean for an ecoregion was divided by the standard deviation across the previous 16-year period, assuming a normal distribution of fire density over time in the ecoregion. The result for each ecoregion was a standardized z-score, which is a dimensionless quantity describing the degree to which the fire occurrence density in the ecoregion in 2017 was higher, lower, or the same relative to all the previous years for which data have been collected, accounting for the variability in the previous years. The z-score is the number of standard deviations between the observation and the mean of the historic observations in the previous years.

Approximately 68 percent of observations would be expected within one standard deviation of the mean, and 95 percent within two standard deviations. Near-normal conditions are classified as those within a single standard deviation of the mean, although such a threshold is somewhat arbitrary. Conditions between about one and two standard deviations of the mean are moderately different from mean conditions, but are not significantly different statistically. Those outside about two standard deviations would be considered statistically greater than or less than the long-term mean (at $p < 0.025$ at each tail of the distribution).

Additionally, we used the Spatial Association of Scalable Hexagons (SASH) analytical approach to identify forested areas in the conterminous United States with higher-than-expected fire occurrence density in 2017. This method identifies locations where ecological phenomena occur at greater or lower occurrences than expected by random chance and is based on a sampling frame optimized for spatial neighborhood analysis, adjustable to the appropriate spatial resolution, and applicable to multiple data types (Potter and others 2016). Specifically, it consists of dividing an analysis area into scalable equal-area hexagonal cells within which data are aggregated, followed by identifying statistically significant geographic clusters of hexagonal cells within which mean

values are greater or less than those expected by chance. To identify these clusters, we employed a Getis-Ord G_i^* hot spot analysis (Getis and Ord 1992) in ArcMap[®] 10.3 (ESRI 2015).

The spatial units of analysis were 9,810 hexagonal cells, each approximately 834 km² in area, generated in a lattice across the conterminous United States using intensification of the Environmental Monitoring and Assessment Program (EMAP) North American hexagon coordinates (White and others 1992). These coordinates are the foundation of a sampling frame in which a hexagonal lattice was projected onto the conterminous United States by centering a large base hexagon over the region (Reams and others 2005, White and others 1992). This base hexagon can be subdivided into many smaller hexagons, depending on sampling needs, and serves as the basis of the plot sampling frame for the Forest Inventory and Analysis (FIA) program (Reams and others 2005). Importantly, the hexagons maintain equal areas across the study region regardless of the degree of intensification of the EMAP hexagon coordinates. In addition, the hexagons are compact and uniform in their distance to the centroids of neighboring hexagons, meaning that a hexagonal lattice has a higher degree of isotropy (uniformity in all directions) than does a square grid (Shima and others 2010). These are convenient and highly useful attributes for spatial neighborhood

analyses. These scalable hexagons also are independent of geopolitical and ecological boundaries, avoiding the possibility of different sample units (such as counties, States, or watersheds) encompassing vastly different areas (Potter and others 2016). We selected hexagons 834 km² in area because this is a manageable size for making monitoring and management decisions in analyses across the conterminous United States (Potter and others 2016).

Fire occurrence density values for each hexagon were quantified as the number of forest fire occurrences per 100 km² of forested area within the hexagon. The Getis-Ord G_i^* statistic was used to identify clusters of hexagonal cells with fire occurrence density values higher than expected by chance. This statistic allows for the decomposition of a global measure of spatial association into its contributing factors, by location, and is therefore particularly suitable for detecting outlier assemblages of similar conditions in a dataset, such as when spatial clustering is concentrated in one subregion of the data (Anselin 1992).

Briefly, G_i^* sums the differences between the mean values in a local sample, determined in this case by a moving window of each hexagon and its 18 first- and second-order neighbors (the 6 adjacent hexagons and the 12 additional hexagons contiguous to those 6) and the global mean of the 7,595 forested hexagonal cells (of

the total 9,810) in the conterminous United States. As described in Laffan (2006), it is calculated as

$$G_i^*(d) = \frac{\sum_j w_{ij}(d)x_j - W_i^* \bar{x}^*}{s^* \sqrt{\frac{(ns_{1i}^*) - W_i^{*2}}{n-1}}}$$

where

G_i^* = the local clustering statistic (in this case, for the target hexagon)

i = the center of local neighborhood (the target hexagon)

d = the width of local sample window (the target hexagon and its first- and second-order neighbors)

x_j = the value of neighbor j

w_{ij} = the weight of neighbor j from location i (all the neighboring hexagons in the moving window were given an equal weight of 1)

n = number of samples in the dataset (the 7,595 forested hexagons)

W_i^* = the sum of the weights

s_{1i}^* = the number of samples within d of the central location (19: the focal hexagon and its 18 first- and second-order neighbors)

\bar{x}^* = the mean of whole dataset (in this case, for all 7,595 forested hexagons)

s^* = the standard deviation of whole dataset (for all 7,595 forested hexagons)

G_i^* is standardized as a z-score with a mean of 0 and a standard deviation of 1, with values >1.96 representing significant local clustering of higher fire occurrence densities ($p < 0.025$) and values <-1.96 representing significant clustering of lower fire occurrence densities ($p < 0.025$), because 95 percent of the observations under a normal distribution should be within approximately two standard deviations of the mean (Laffan 2006). Values between -1.96 and 1.96 have no statistically significant concentration of high or low values; a hexagon and its 18 neighbors, in other words, have a normal range of both high and low numbers of fire occurrences per 100 km² of forested area. It is worth noting that the threshold values are not exact because the correlation of spatial data violates the assumption of independence required for statistical significance (Laffan 2006). In addition, the Getis-Ord approach does not require that the input data be normally distributed, because the local G_i^* values are computed under a randomization assumption, with G_i^* equating to a standardized z-score that asymptotically tends to a normal distribution (Anselin 1992). The z-scores are considered to be reliable, even with skewed data, as long as the local neighborhood encompasses several observations (ESRI 2015), in this case, via the target hexagon and its 18 first- and second-order neighbors.

RESULTS AND DISCUSSION

Trends in Forest Fire Occurrence Detections for 2017

The MODIS Active Fire database recorded 92,864 forest fire occurrences across the conterminous United States in 2017, the fifth most in 17 full years of data collection and the most since 2014 (fig. 3.1). This was approximately 95 percent more than in 2016 (47,744 total forest fire occurrences), and about 43 percent higher than the annual mean of 64,913 forest fire occurrences across the previous 16 years of data collection. In Alaska, meanwhile, the MODIS database captured 2,043 forest fire occurrences in 2017, about 7 percent less than the preceding year (2,196) and about 82 percent less than the previous 16-year annual

mean of 11,317. Meanwhile, Hawaii had 118 fire occurrences in 2017, a decrease of about 90 percent from the previous year (1,210) and 72 percent below the average of 426 fire occurrences over the previous 16 years. Finally, 10 forest fire occurrences were detected in Puerto Rico, 27 percent fewer than the previous average of 13.7 per year.

The increase in the total number of fire occurrences across the United States is generally consistent with the official wildland fire statistics (National Interagency Coordination Center 2018). In 2017, 71,499 wildland fires were reported across the United States, an increase from 67,743 in 2016. At the same time, the area burned nationally (4 057 413 ha) was 153 percent above the 10-year annual average

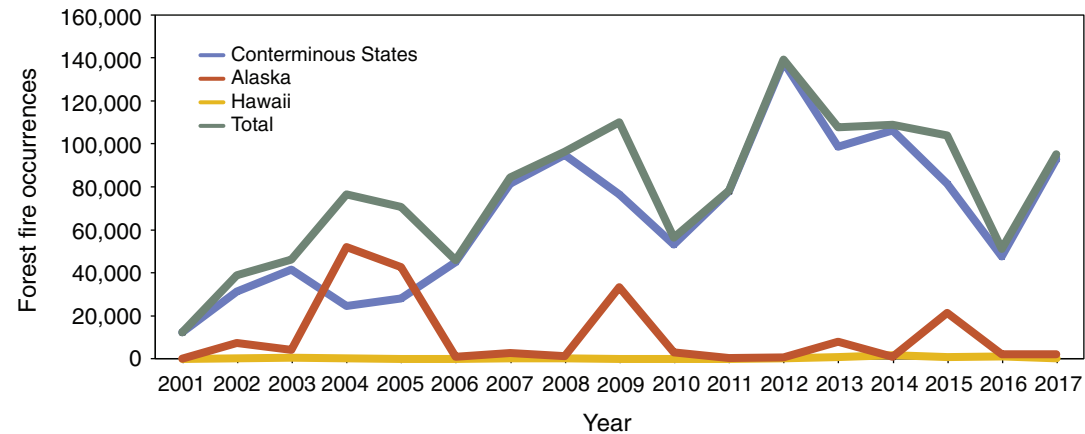


Figure 3.1—Forest fire occurrences detected by MODIS from 2001 to 2017 for the conterminous United States, Alaska, and Hawaii, and for the entire Nation combined. (Data source: U.S. Department of Agriculture Forest Service, Remote Sensing Applications Center, in conjunction with the NASA MODIS Rapid Response group)

and 73 percent greater than the area burned in 2016 (2 339 815 ha) (National Interagency Coordination Center 2017, 2018). Also in 2017, 44 wildland fires and fire complexes exceeded 16 187 ha, compared to 19 in 2016 and 52 in 2015 (National Interagency Coordination Center 2017, 2018). As noted in the Methods section, estimates of burned area are different metrics for quantifying fire activity than calculations of MODIS-detected fire occurrences, though the two may be correlated.

Areas with the highest fire occurrence densities were in the Pacific Northwest region and in California (fig. 3.2). Precipitation was above normal in these areas early in 2017, promoting significant growth of fine fuels; July and August were then very dry in many areas, except in central and southern parts of California, which dried considerably later in the year with the lack of autumn rain combined with strong winds (National Interagency Coordination Center 2018). The ecoregion section with the highest fire occurrence density by far was M332B–Northern Rockies and Bitterroot Valley in western Montana, with 41.8 fire occurrences/100 km² of forest (table 3.1). This was the location of the Rice Ridge Fire, a lightning-ignited fire that burned 64 825 ha between July 24 and October 17 and cost approximately \$49.3 million in damages and containment (National Interagency Coordination Center 2018). Fire occurrence densities were also very high in M261A–Klamath Mountains in northwestern California and southwestern Oregon (27.9 fire occurrences/100 km² of

forest), location of the Chetco Bar Fire, which scorched 77 346 ha from its lightning ignition on July 12 until October 26 and cost approximately \$72 million to contain (National Interagency Coordination Center 2018). Two other ecoregion sections experienced >20 fires/100 km² of forest: M333C–Northern Rockies (22.0) and 261B–Southern California Coast (20.7) (table 3.1). The latter of these was the site of the 109 265-ha Thomas Fire, which burned in Ventura and Santa Barbara Counties from December 4 through the end of the year and cost at least \$123.8 million (National Interagency Coordination Center 2018). This was the largest wildfire in recorded California history (CAL FIRE 2018).

Fire occurrence densities were also comparatively quite high (12.1–24 fire occurrences/100 km² of forest) throughout the Cascade Range of Washington and Oregon (M242D–Northern Cascades and M242B–Western Cascades) and in parts of the northern Rockies in central and northern Idaho and western Montana (M332A–Idaho Batholith and M333D–Bitterroot Mountains) (fig. 3.2).

Other ecoregion sections in the Southeast and scattered throughout the West had moderately high fire occurrence densities (6.1–12 fire occurrences/100 km² of forest) (fig. 3.2). In the Southeast, this included an area from southern Mississippi along the Gulf Coast (232B–Gulf Coastal Plains and Flatwoods) and northeast through Georgia and South Carolina into North Carolina (232J–Southern Atlantic Coastal Plains and Flatwoods). Fire occurrence densities

Table 3.1—The 15 ecoregion sections in the conterminous United States with the highest fire occurrence densities in 2017

Section	Name	Forest area <i>km</i> ²	Fire occurrences	Density
M332B	Northern Rockies and Bitterroot Valley	158.8	6,643	41.8
M261A	Klamath Mountains	343.1	9,566	27.9
M333C	Northern Rockies	172.7	3,807	22.0
261B	Southern California Coast	40.7	843	20.7
M332A	Idaho Batholith	361.0	7,007	19.4
M242D	Northern Cascades	230.7	3,374	14.6
M242B	Western Cascades	417.7	6,041	14.5
M333D	Bitterroot Mountains	222.9	2,850	12.8
M333B	Flathead Valley	160.6	1,575	9.8
263A	Northern California Coast	123.2	1,184	9.6
322C	Colorado Desert	0.4	4	9.1
M261F	Sierra Nevada Foothills	71.2	626	8.8
M261E	Sierra Nevada	438.1	3,708	8.5
232J	Southern Atlantic Coastal Plains and Flatwoods	439.5	3,551	8.1
232B	Gulf Coastal Plains and Flatwoods	732.3	5,664	7.7

were also moderately high in two neighboring ecoregion sections in Arkansas and Oklahoma: 231G–Arkansas Valley and 255A–Cross Timbers and Prairie.

Additionally, moderately high fire occurrence densities were recorded in several Western ecoregion sections, all with 6.1–12 fire occurrences/100 km² of forest: 321A–Basin and Range, in southeastern Arizona, southern New Mexico, and far western Texas; M261E–Sierra Nevada and M261F–Sierra Nevada Foothills, in California; 263A–Northern California

Coast and M261B–Northern California Coast Ranges; and M333B–Flathead Valley, in northwestern Montana.

Meanwhile, Alaska experienced above-average temperatures, but periodic precipitation events minimized the fire impacts of the heat (National Interagency Coordination Center 2018). Fire occurrence densities were low across the State (fig. 3.3), with the exception of M139B–Olgivie Mountains in eastern Alaska (3.6 fires occurrences/100 km² of forest). This was where the 37 846-ha Campbell River Fire

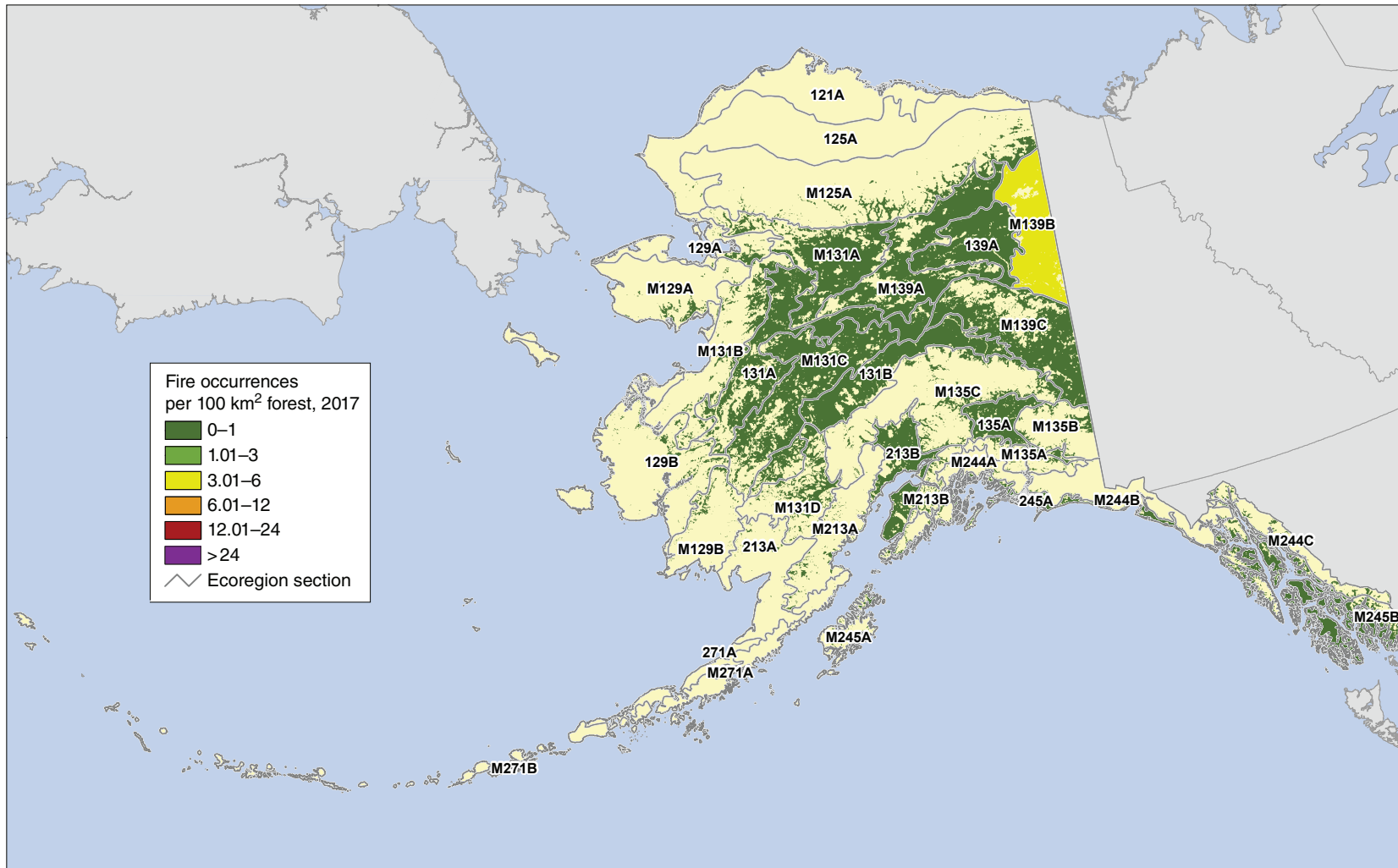


Figure 3.3—The number of forest fire occurrences, per 100 km² (10 000 ha) of forested area, by ecoregion section within Alaska, for 2017. The gray lines delineate ecoregion sections (Nowacki and Brock 1995). Forest cover is derived from MODIS imagery by the Forest Service Remote Sensing Applications Center. (Source of fire data: U.S. Department of Agriculture Forest Service, Remote Sensing Applications Center, in conjunction with the NASA MODIS Rapid Response group)

burned from late June into early October, extending well into the neighboring Yukon Territory of Canada.

In Hawaii, lava flows from the 35-year-long eruption of Pu'u 'Ō'ō, a vent on the flank of the Kīlauea volcano on the Big Island, continued to be the cause of most forest fire occurrences. Fire occurrence density on the Big Island was 2.9/100 km² of forest in 2017 (fig. 3.4), one-tenth of the 29.6 fire occurrences/100 km² of forest recorded in 2016 (Potter 2018). All the other islands in the archipelago experienced <1 fire occurrence/100 km² of forest.

Finally, all of the islands constituting the U.S. Caribbean territories had <1 fire occurrence/100 km² of forest in 2017 (fig. 3.5).

Comparison to Longer Term Trends

The nature of the MODIS Active Fire data makes it possible to contrast, for each ecoregion section and Hawaiian and Caribbean island, short-term (1-year) forest fire occurrence densities with longer term trends encompassing the first 16 full years of data collection (2001–2016). In general, the ecoregion sections with the highest annual fire occurrence means are located in the northern Rocky Mountains, the Southwest, California, Oklahoma, and the Gulf Coastal Plain, while most ecoregion sections

within the Northeastern, Midwestern, Middle Atlantic, and Appalachian regions experienced <1 fire occurrence/100 km² of forest annually during the multiyear period (fig. 3.6A). The forested ecoregion section that experienced the most fire occurrences each year on average was M332A–Idaho Batholith in central Idaho (mean annual fire occurrence density of 13.0) (table 3.2), which also had a high fire occurrence density in 2017. Other ecoregion sections with high mean fire occurrence densities (6.1–12.0 fire occurrences/100 km² of forest) were located along the Gulf Coast in the Southeast; in coastal, northern, and central areas of California; in central Arizona and New Mexico; in the northern Rocky Mountains; and in central Oklahoma (table 3.2). The ecoregion section with the greatest variation in fire occurrence densities from 2001 to 2016 was M332A–Idaho Batholith, with more moderate variation in California, northern Washington, southern and northeastern Oregon, western Montana, central Arizona and west-central New Mexico, and eastern North Carolina (fig. 3.6B). Less variation occurred throughout the central and northern Rocky Mountain States, the Southeast, and central Oregon and Washington. The lowest levels of variation occurred throughout most of the Midwest and Northeast.

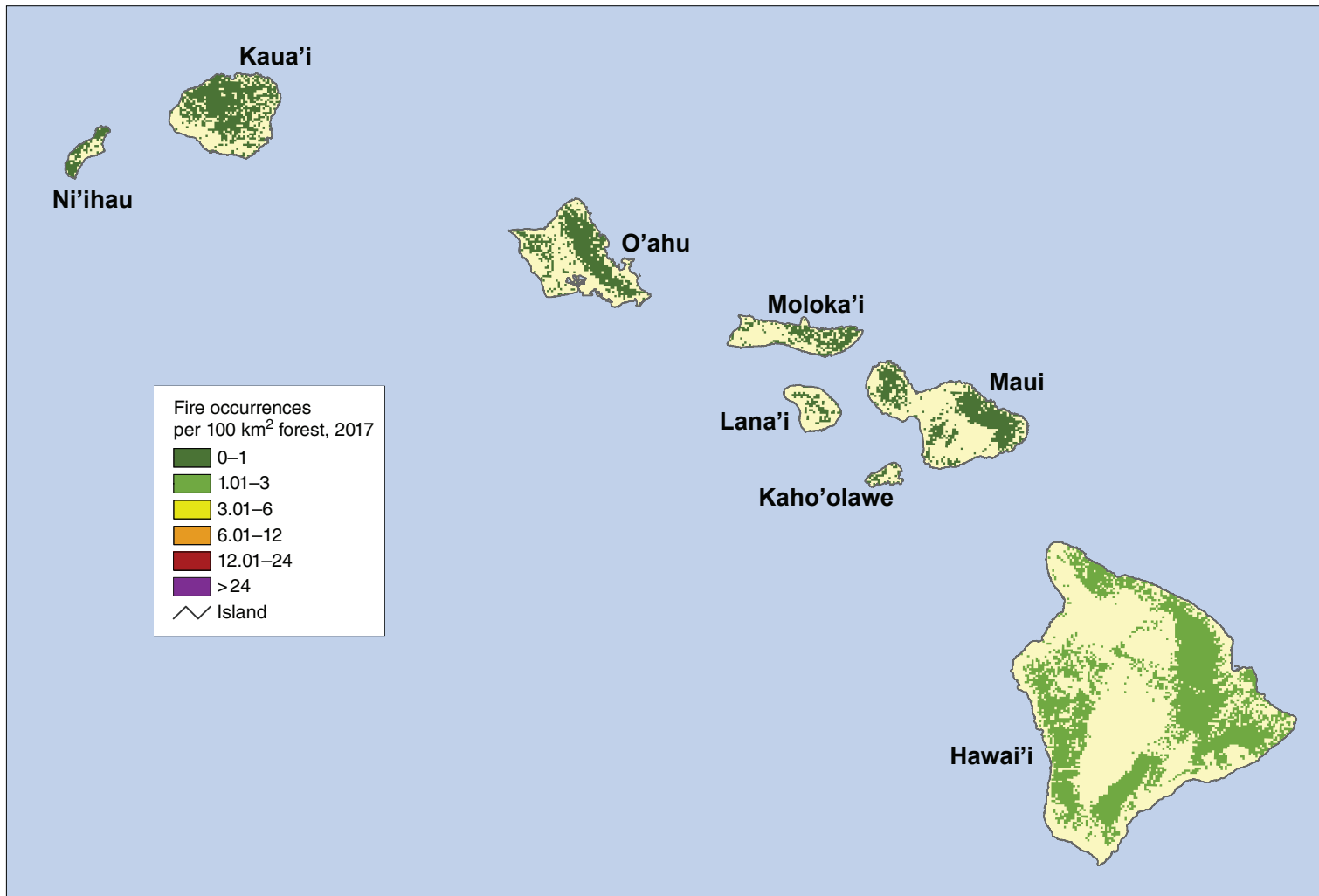


Figure 3.4—The number of forest fire occurrences, per 100 km² (10 000 ha) of forested area, by island in Hawaii, for 2017. Background forest cover is derived from the LANDFIRE program (LANDFIRE 2014). (Source of fire data: U.S. Department of Agriculture Forest Service, Remote Sensing Applications Center, in conjunction with the NASA MODIS Rapid Response group)

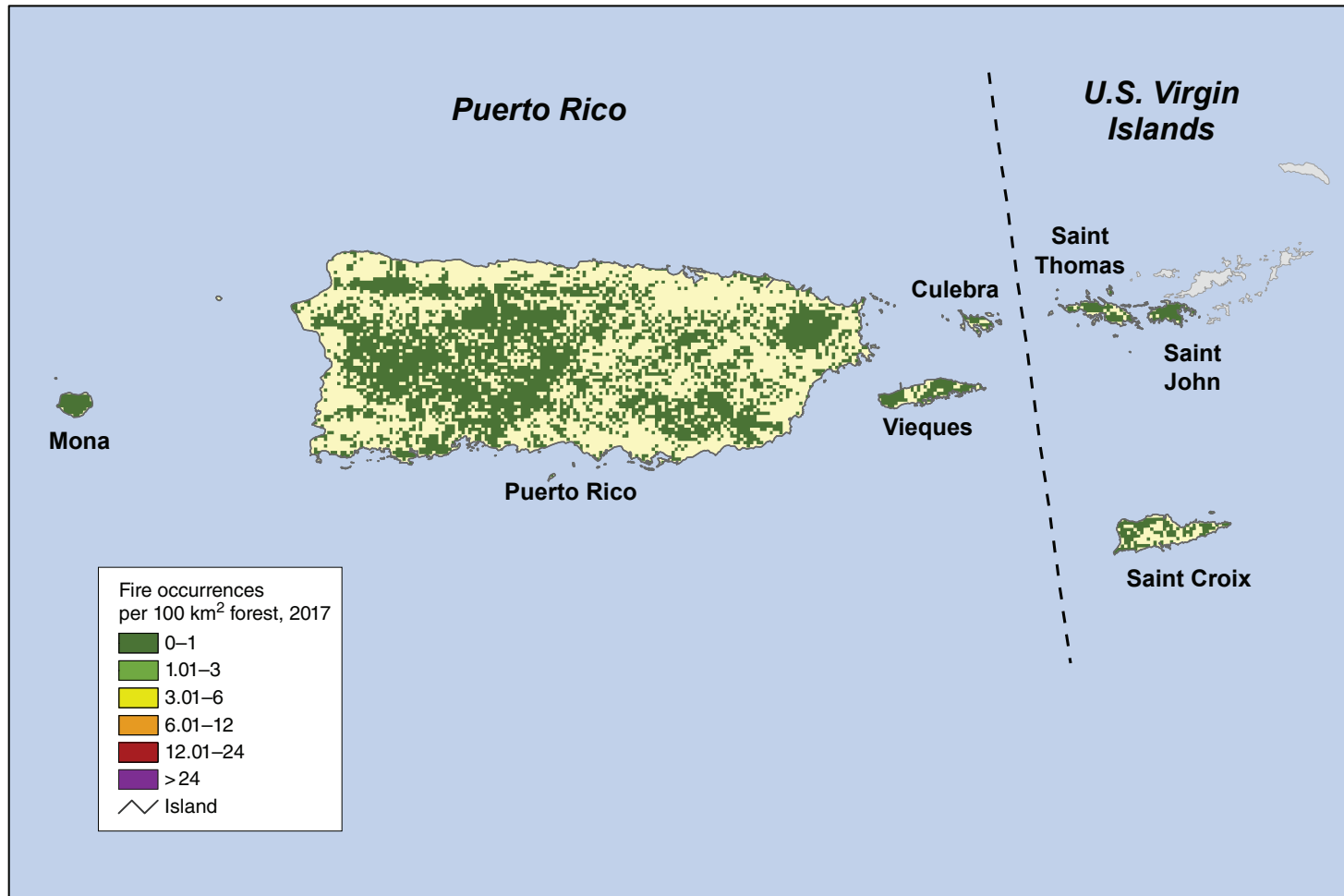


Figure 3.5—The number of forest fire occurrences, per 100 km² (10 000 ha) of forested area, by island in Puerto Rico and the U.S. Virgin Islands, for 2017. Forest cover is from the Forest Service International Institute of Tropical Forestry, derived from a cloud-free Landsat image mosaic developed in cooperation with Forest Service Remote Sensing Applications Center (Kennaway and Helmer 2007, Kennaway and others 2008).

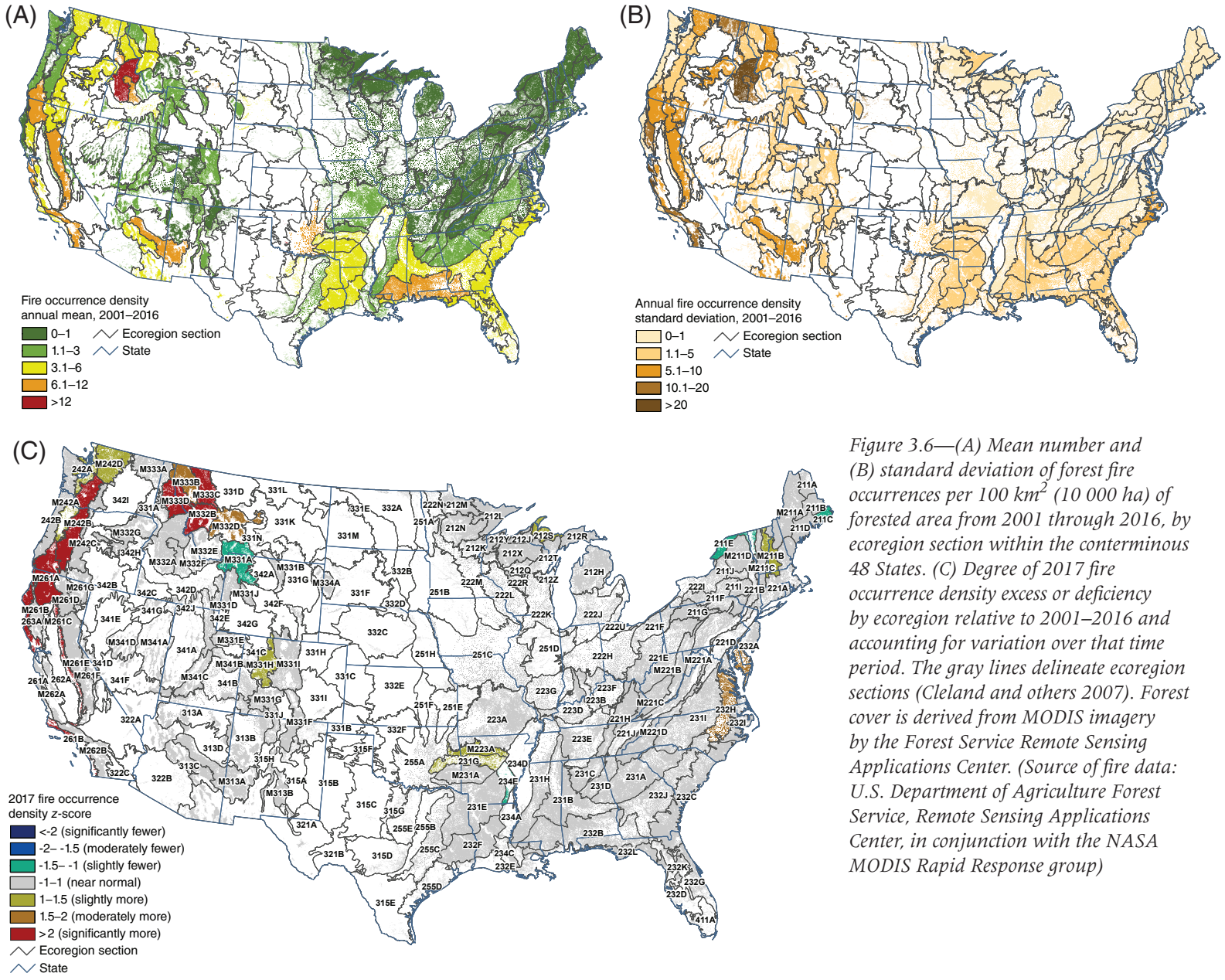


Figure 3.6—(A) Mean number and (B) standard deviation of forest fire occurrences per 100 km² (10 000 ha) of forested area from 2001 through 2016, by ecoregion section within the conterminous 48 States. (C) Degree of 2017 fire occurrence density excess or deficiency by ecoregion relative to 2001–2016 and accounting for variation over that time period. The gray lines delineate ecoregion sections (Cleland and others 2007). Forest cover is derived from MODIS imagery by the Forest Service Remote Sensing Applications Center. (Source of fire data: U.S. Department of Agriculture Forest Service, Remote Sensing Applications Center, in conjunction with the NASA MODIS Rapid Response group)

Table 3.2—The 14 ecoregion sections in the conterminous United States with the highest annual mean fire occurrence densities from 2001 through 2016

Section	Name	Forest area <i>km²</i>	Mean annual fire occurrence density
332F	South Central and Red Bed Plains	1.5	18.4
M332A	Idaho Batholith	361.0	13.0
331G	Powder River Basin	6.2	10.3
261A	Central California Coast	58.3	9.7
M262B	Southern California Mountain and Valley	155.3	8.6
251F	Flint Hills	0.8	7.8
322C	Colorado Desert	0.4	7.8
M261E	Sierra Nevada	438.1	7.6
M261A	Klamath Mountains	343.1	6.9
331A	Palouse Prairie	28.3	6.6
255A	Cross Timbers and Prairie	79.0	6.4
232B	Gulf Coastal Plains and Flatwoods	732.3	6.3
M313A	White Mountains-San Francisco Peaks-Mogollon Rim	386.7	6.1
M332F	Challis Volcanics	90.0	6.1

As determined by the calculation of standardized fire occurrence z-scores, ecoregion sections in southern, central, and northern California; the Cascade Mountains of Oregon and Washington; and northern Idaho and northwestern Montana experienced significantly greater fire occurrence densities than normal in 2017, compared to the previous 16-year mean and accounting for variability over time (fig. 3.6C). The ecoregion section with the highest fire occurrence density in 2017 (M332B—Northern Rockies and Bitterroot Valley, fig. 3.2) also had a high z-score. Additionally, some

ecoregion sections had moderately or slightly higher fire occurrence density than expected as shown by their z-scores (fig. 3.6C), including 232H—Middle Atlantic Coastal Plains and Flatwoods in eastern North Carolina, Virginia, and the Delmarva Peninsula; M223A—Boston Mountains and 231G—Arkansas Valley in northern Arkansas and eastern Oklahoma; 212S—Northern Upper Peninsula in Michigan; M211B—New England Piedmont in Vermont and New Hampshire; and M331H—North-Central Highlands and Rocky Mountains in central Colorado.

A handful of ecoregion sections across the country had lower fire occurrence densities in 2017 compared to the longer term as indicated by their z-scores: M331A–Yellowstone Highlands in northwestern Wyoming, southwestern Montana, and northeastern Idaho; 234E–Arkansas Alluvial Plains in southeastern Arkansas; 211E–St. Lawrence and Champlain Valley in northern New York and Vermont; and 211C–Fundy Coastal and Interior in southeastern Maine. All had very low fire occurrence densities in 2017, and low or relatively low annual mean fire occurrence density and variation from 2001–2016.

In Alaska, meanwhile, moderate mean fire occurrence density existed in the east-central and central parts of the State centered on the 139A–Yukon Flats ecoregion section and including M139A–Ray Mountains, M139B–Olgivie Mountains, and M139C–Dawson Range (fig. 3.7A). These same areas experienced the greatest degree of variability over the 16-year period preceding 2017 (fig. 3.7B). In 2017, only one ecoregion section, M213B–Kenai Mountains, was outside the range of near-normal fire occurrence density (z -score >2), having many more fire occurrences compared to the mean of the previous 16 years and accounting for variability (fig. 3.7C).

In Hawaii, both mean annual fire occurrence density (fig. 3.8A) and variability (fig. 3.8B) were highest on the Big Island during the

2001–2016 period. The annual mean was <1 fire occurrence/100 km² of forest for all islands except the Big Island (12.7) and Kaho‘olawe (1.7). The annual fire occurrence standard deviation exceeded 1 for only the Big Island (17.7), Kaho‘olawe (5.1), and Lāna‘i (1.2). No Hawaiian island in 2017 was outside the range of near-normal fire occurrence density, controlling for variability over the previous 16 years (z -score between -1 and 1) (fig. 3.7C).

All the islands of the Caribbean territories had annual fire occurrence means and standard deviations <1 (figs. 3.9A and 3.9B). Additionally, each of the islands was within the range of near-normal fire occurrence density (z -score between -1 and 1) (fig. 3.9C).

Geographical Hot Spots of Fire Occurrence Density

Although summarizing fire occurrence data at the ecoregion section scale allows for the quantification of fire occurrence density across the country, a geographical hot spot analysis can offer insights into where, statistically, fire occurrences are more concentrated than expected by chance. In 2017, the SASH method detected three geographical hot spots of very high fire occurrence density ($G_i^* >12$ and ≤ 24) (fig. 3.10). These corresponded with areas of high fire occurrence density (fig. 3.2), including M332B–Northern Rockies and Bitterroot Valley and M261A–Klamath Mountains (see above), as well as M332A–Idaho Batholith.

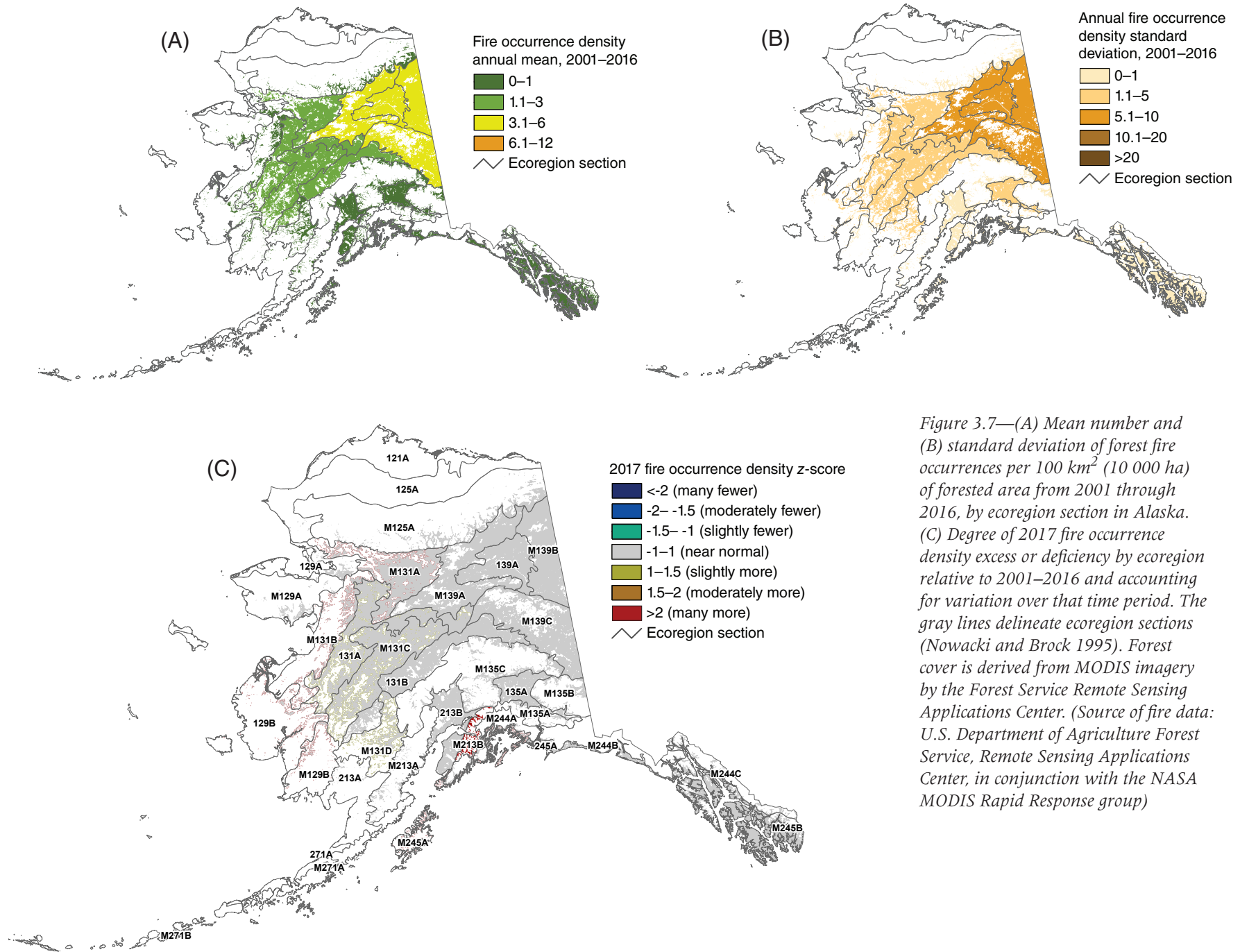


Figure 3.7—(A) Mean number and (B) standard deviation of forest fire occurrences per 100 km² (10 000 ha) of forested area from 2001 through 2016, by ecoregion section in Alaska. (C) Degree of 2017 fire occurrence density excess or deficiency by ecoregion section relative to 2001–2016 and accounting for variation over that time period. The gray lines delineate ecoregion sections (Nowacki and Brock 1995). Forest cover is derived from MODIS imagery by the Forest Service Remote Sensing Applications Center. (Source of fire data: U.S. Department of Agriculture Forest Service, Remote Sensing Applications Center, in conjunction with the NASA MODIS Rapid Response group)

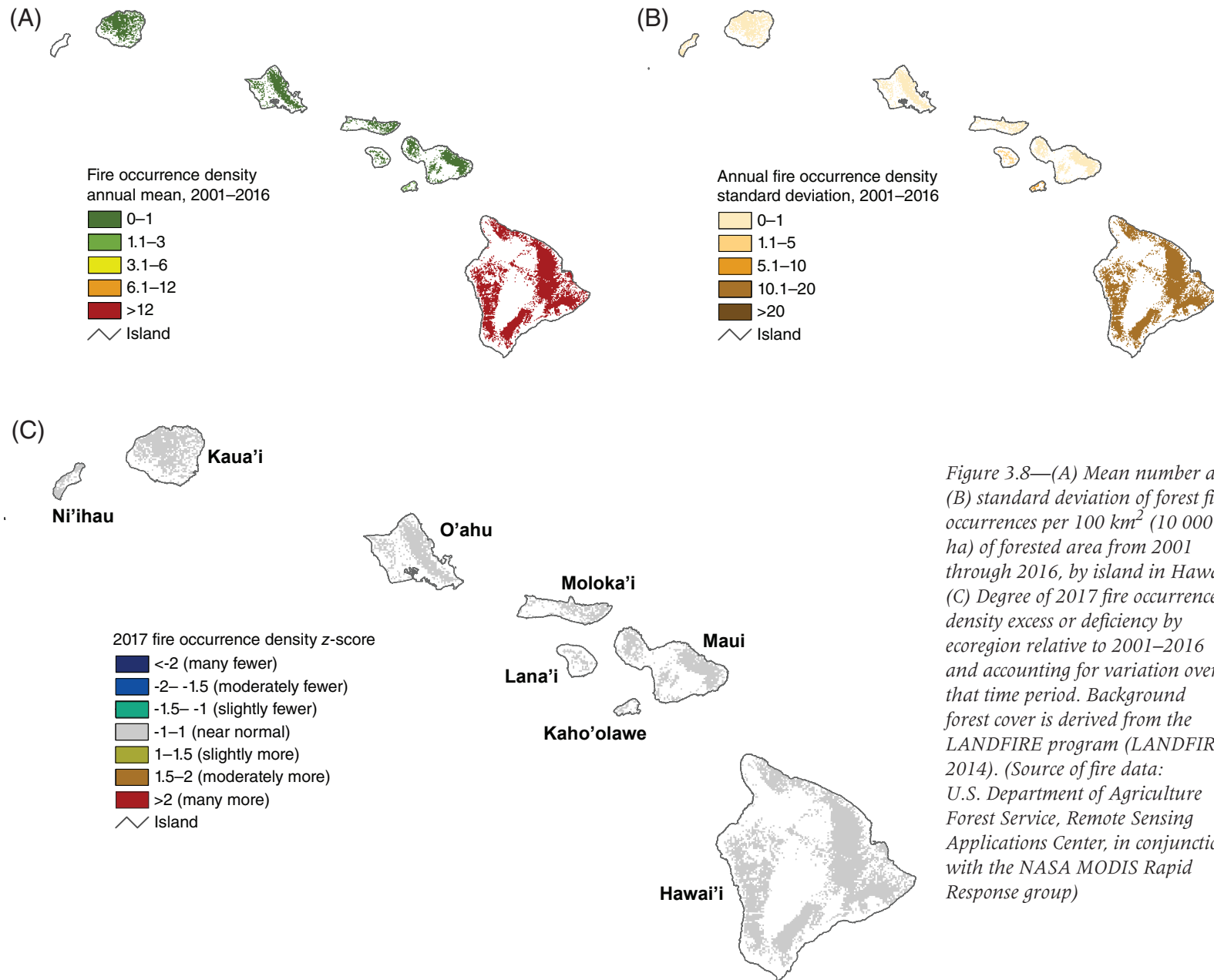


Figure 3.8—(A) Mean number and (B) standard deviation of forest fire occurrences per 100 km² (10 000 ha) of forested area from 2001 through 2016, by island in Hawaii. (C) Degree of 2017 fire occurrence density excess or deficiency by ecoregion relative to 2001–2016 and accounting for variation over that time period. Background forest cover is derived from the LANDFIRE program (LANDFIRE 2014). (Source of fire data: U.S. Department of Agriculture Forest Service, Remote Sensing Applications Center, in conjunction with the NASA MODIS Rapid Response group)

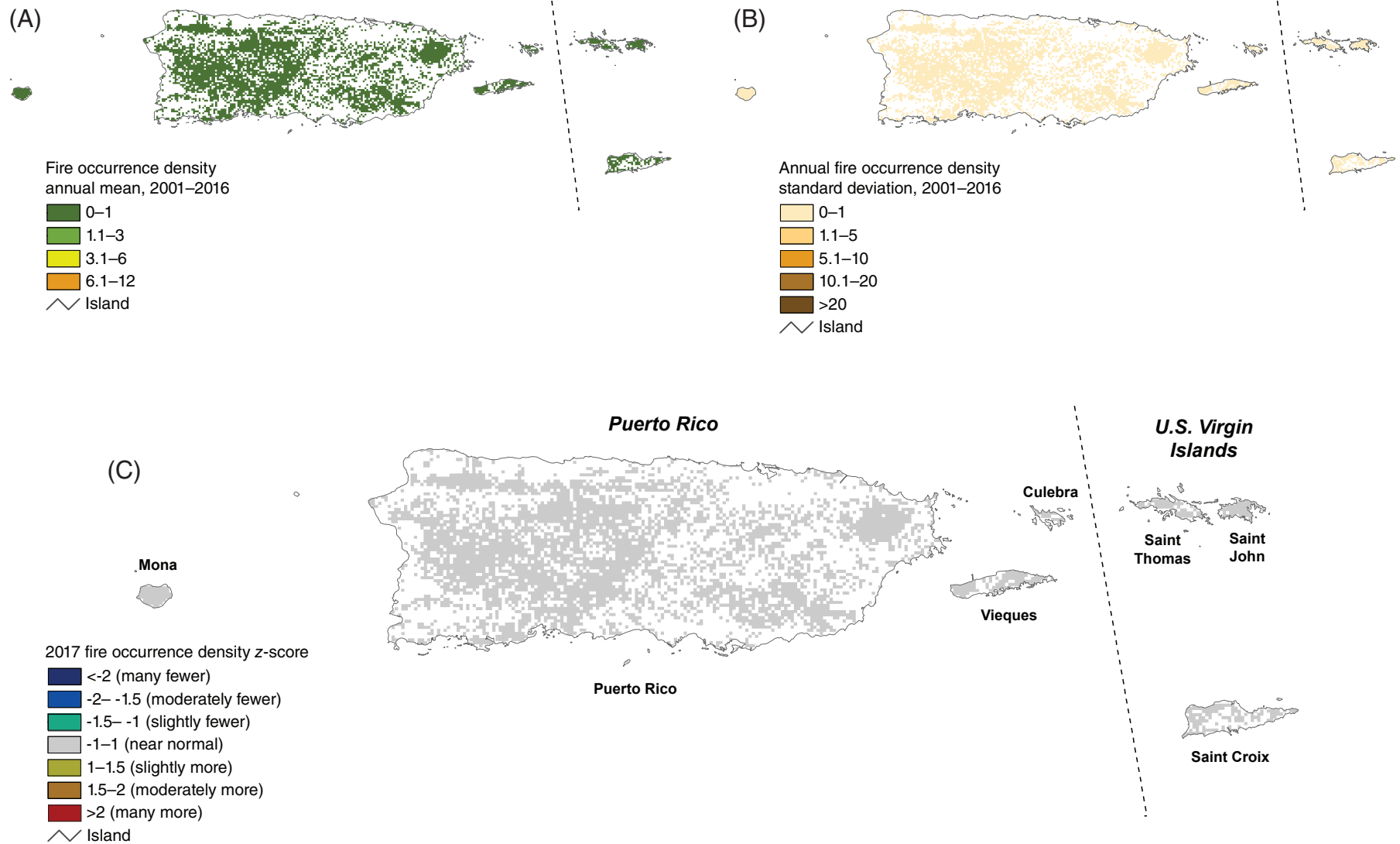


Figure 3.9—(A) Mean number and (B) standard deviation of forest fire occurrences per 100 km² (10 000 ha) of forested area from 2001 through 2016, by island in Puerto Rico and the U.S. Virgin Islands. (C) Degree of 2017 fire occurrence density excess or deficiency by ecoregion relative to 2001–2016 and accounting for variation over that time period. Forest cover is from the Forest Service International Institute of Tropical Forestry (IITF), derived from a cloud-free Landsat image mosaic developed in cooperation with Forest Service Remote Sensing Applications Center (Kennaway and Helmer 2007, Kennaway and others 2008).

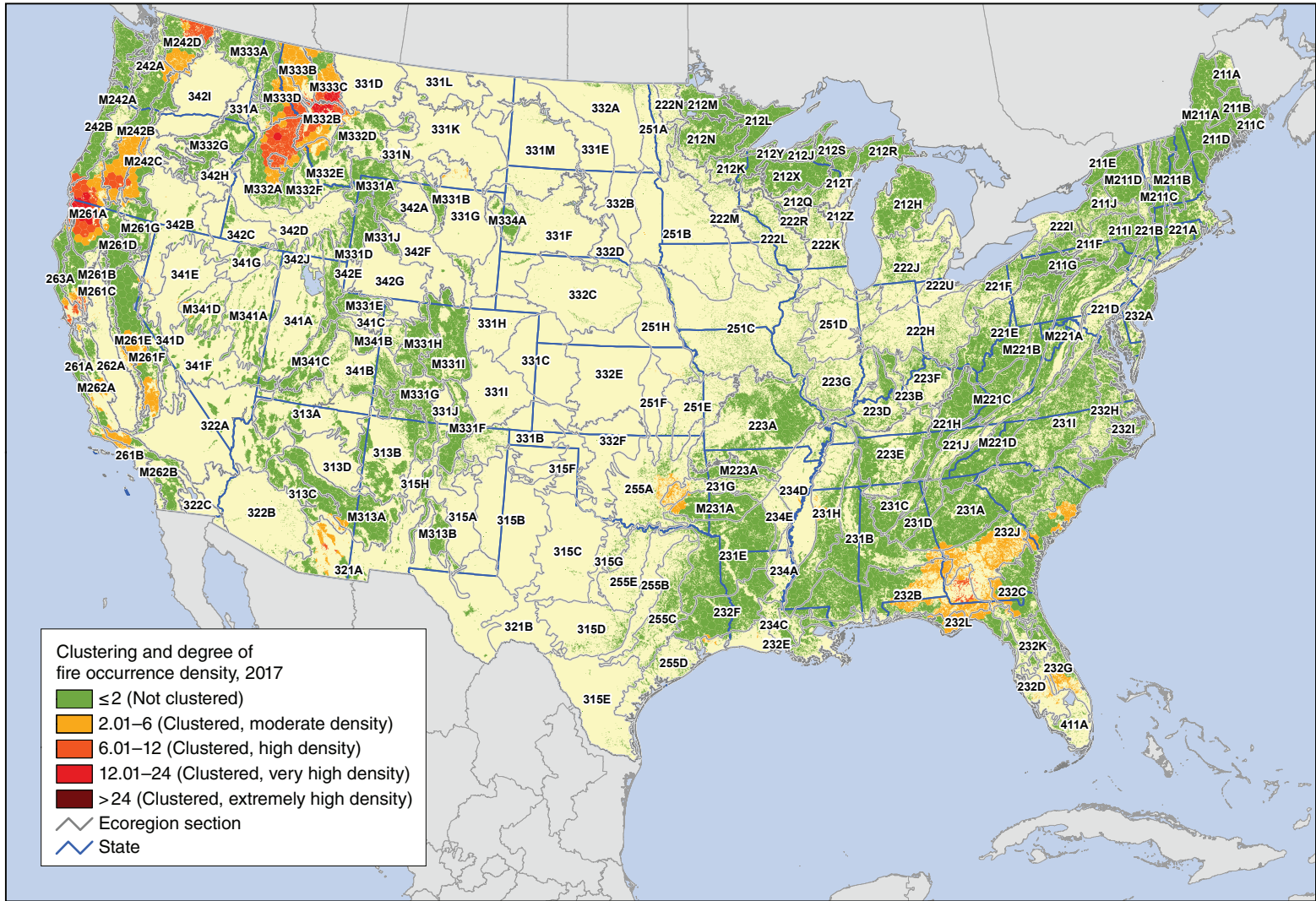


Figure 3.10—Hot spots of fire occurrence across the conterminous United States for 2017. Values are Getis-Ord G_i^* scores, with values >2 representing significant clustering of high fire occurrence densities. (No areas of significant clustering of lower fire occurrence densities, <-2 , were detected.) The gray lines delineate ecoregion sections (Cleland and others 2007). Background forest cover is derived from MODIS imagery by the Forest Service Remote Sensing Applications Center. (Source of fire data: U.S. Department of Agriculture Forest Service, Remote Sensing Applications Center, in conjunction with the NASA MODIS Rapid Response group)

Meanwhile, four hot spots of high fire occurrence density ($G_i^* > 6$ and ≤ 12) were identified in the West, along with one in the East (fig. 3.10). One of these was in coastal California north of San Francisco Bay (in 263A–Northern California Coast, M261B–Northern California Coast Ranges, and M261C–Northern California Interior Coast Ranges), where several wildfires in October burned >99 000 ha, killing 44 and destroying 8,900 structures. It was the costliest wildfire complex in U.S. history, resulting in \$9 billion in insurance claims (Cooper 2017).

The SASH analysis also detected a geographic hot spot (G_i^*) of high fire occurrence density in north-central Washington (M242D–Northern Cascades). This is where the Diamond Creek Fire scorched 51 910 ha between July 23 and October 5, costing \$14.8 million in damages and containment. Other hot spots of similar intensity were located in southern Oregon (M242B–Western Cascades and M242C–Eastern Cascades), southeastern Arizona (321A–Basin and Range), and southwestern Georgia (232B–Gulf Coastal Plains and Flatwoods).

Hot spots of moderate fire density in 2017 ($G_i^* > 2$ and ≤ 6) were scattered elsewhere near the West Coast and in the Southeastern United States (fig. 3.10), including in the following regions:

- Southern California (261B–Southern California Coast, M262B–Southern California Mountain and Valley, and M261E–Sierra Nevada)

- Central California (two in M261E–Sierra Nevada and one in M262A–Central California Coast Ranges)
- Central Nevada (M341D–West Great Basin and Mountains)
- Central Washington (M242D–Northern Cascades, M242B–Western Cascades, and M242C–Eastern Cascades)
- Eastern Oklahoma (255A–Cross Timbers and Prairie, 231G–Arkansas Valley, and M231A–Ouachita Mountains)
- Southeastern Texas (232F–Coastal Plains and Flatwoods–Western Gulf and 232E–Louisiana Coastal Prairie and Marshes)
- Southern Florida (232D–Florida Coastal Lowlands–Gulf and 232G–Florida Coastal Lowlands–Gulf)
- Coastal Plain of South Carolina (232C–Atlantic Coastal Flatwoods)

CONCLUSIONS AND FUTURE WORK

In 2017, the number of MODIS satellite-detected forest fire occurrences recorded for the conterminous States was the fifth most in 17 full years of data collection and the most since 2014. Ecoregion sections in the Pacific Northwest, the northern Rocky Mountains, and California had the highest forest fire occurrence density per 100 km² of forested area. Geographic hot spots of high fire occurrence density were detected in these same areas, as well as in the Southeast and southern Arizona. Ecoregion sections in southern, central, and northern California; the Cascade Mountains of Oregon and Washington; and northern Idaho and northwestern Montana

experienced greater fire occurrence density than normal compared to the previous 16-year mean and accounting for variability over time. Alaska experienced low fire occurrence densities except in one northeastern ecoregion section. The Big Island of Hawai'i experienced a lower fire occurrence density than in recent years as a result of an ongoing volcanic eruption.

The results of these geographic analyses are intended to offer insights into where fire occurrences have been concentrated spatially in a given year and compared to previous years, but are not intended to quantify the severity of a given fire season. Given the limits of MODIS active fire detection using 1-km resolution data, these products also may underrepresent the number of fire occurrences in some ecosystems where small and low-intensity fires are common, and where high cloud frequency can interfere with fire detection. These products can also have commission errors. However, these high temporal fidelity products currently offer the best means for daily monitoring of forest fire occurrences.

Future work related to understanding geographic patterns of forest fire occurrences in the United States could include a comparison of the MODIS detections with those of the VIIRS sensor, an analysis of fire occurrence detections by forest cover types, an evaluation of whether the fire occurrences correspond with mapped burned areas, and an assessment of the relationships between fire occurrence and drought conditions.

Ecological and forest health impacts relating to fire and other abiotic disturbances are scale-dependent properties, which in turn are affected by management objectives (Lundquist and others 2011). Information about the concentration of fire occurrences may help pinpoint areas of concern for aiding management activities and for investigations into the ecological and socioeconomic impacts of forest fire potentially outside the range of historic frequency.

LITERATURE CITED

- Anselin, L. 1992. Spatial data analysis with GIS: an introduction to application in the social sciences. Gen. Tech. Rep. 92-10. Santa Barbara, CA: National Center for Geographic Information and Analysis. 53 p.
- Barbour, M.G.; Burk, J.H.; Pitts, W.D. [and others]. 1999. Terrestrial plant ecology. Menlo Park, CA: Addison Wesley Longman, Inc. 649 p.
- Bond, W.J.; Keeley, J.E. 2005. Fire as a global "herbivore": the ecology and evolution of flammable ecosystems. *Trends in Ecology & Evolution*. 20(7): 387–394.
- Brooks, M.L.; D'Antonio, C.M.; Richardson, D.M. [and others]. 2004. Effects of invasive alien plants on fire regimes. *BioScience*. 54(7): 677–688.
- CAL FIRE. 2018. Top 20 largest California wildfires. Jan. 12, 2018. http://www.fire.ca.gov/communications/downloads/fact_sheets/Top20_Acres.pdf. [Date accessed: May 18, 2018].
- Cleland, D.T.; Freeouf, J.A.; Keys, J.E. [and others]. 2007. Ecological subregions: sections and subsections for the conterminous United States. Gen. Tech. Rep. WO-76D. Washington, DC: U.S. Department of Agriculture Forest Service. Map; Sloan, A.M., cartographer; presentation scale 1:3,500,000; colored. Also on CD-ROM as a GIS coverage in ArcINFO format or at <http://data.fs.usda.gov/geodata/edw/datasets.php>. [Date accessed: July 20, 2015].

- Cooper, J.J. 2017. October's Wine Country fires were the costliest ever. Money. Dec. 7, 2017. <http://time.com/money/5054103/octobers-wine-country-fires-were-the-costliest-ever/>. [Date accessed: May 18, 2018].
- Coulston, J.W.; Ambrose, M.J.; Riitters, K.H.; Conkling, B.L. 2005. Forest Health Monitoring 2004 national technical report. Gen. Tech. Rep. SRS-90. Asheville, NC: U.S. Department of Agriculture Forest Service, Southern Research Station. 81 p.
- Edmonds, R.L.; Agee, J.K.; Gara, R.I. 2011. Forest health and protection. Long Grove, IL: Waveland Press, Inc. 667 p.
- ESRI. 2015. ArcMap® 10.3. Redlands, CA: Environmental Systems Research Institute.
- Getis, A.; Ord, J.K. 1992. The analysis of spatial association by use of distance statistics. *Geographical Analysis*. 24(3): 189–206.
- Gill, A.M.; Stephens, S.L.; Cary, G.J. 2013. The worldwide “wildfire” problem. *Ecological Applications*. 23(2): 438–454.
- Hawbaker, T.J.; Radeloff, V.C.; Syphard, A.D. [and others]. 2008. Detection rates of the MODIS active fire product. *Remote Sensing of Environment*. 112: 2656–2664.
- Justice, C.O.; Giglio, L.; Korontzi, S. [and others]. 2002. The MODIS fire products. *Remote Sensing of Environment*. 83(1–2): 244–262.
- Justice, C.O.; Giglio, L.; Roy, D. [and others]. 2011. MODIS-derived global fire products. In: Ramachandran, B.; Justice, C.O.; Abrams, M.J., eds. Land remote sensing and global environmental change: NASA's earth observing system and the science of ASTER and MODIS. New York: Springer: 661–679.
- Kennaway, T.A., Helmer, E.H. 2007. The forest types and ages cleared for land development in Puerto Rico. *GIScience & Remote Sensing*. 44(4): 356–382.
- Kennaway, T.A., Helmer, E.H., Lefsky, M.A. [and others]. 2008. Mapping land cover and estimating forest structure using satellite imagery and coarse resolution lidar in the Virgin Islands. *Journal of Applied Remote Sensing*. 2(1): 023551. DOI: 10.1117/1.3063939.
- Laffan, S.W. 2006. Assessing regional scale weed distributions, with an Australian example using *Nassella trichotoma*. *Weed Research*. 46(3): 194–206.
- LANDFIRE. 2014. Existing vegetation type layer, LANDFIRE 1.4.0. U.S. Department of the Interior, Geological Survey. <https://www.landfire.gov/evt.php>. [Date accessed: May 2, 2014].
- Lundquist, J.E.; Camp, A.E.; Tyrrell, M.L. [and others]. 2011. Earth, wind and fire: abiotic factors and the impacts of global environmental change on forest health. In: Castello, J.D.; Teale, S.A., eds. Forest health: an integrated perspective. New York: Cambridge University Press: 195–243.
- McKenzie, D.; Peterson, D.L.; Alvarado, E. 1996. Predicting the effect of fire on large-scale vegetation patterns in North America. Res. Pap. PNW-489. Portland, OR: U.S. Department of Agriculture Forest Service, Pacific Northwest Research Station. 38 p.
- National Interagency Coordination Center. 2017. Wildland fire summary and statistics annual report: 2016. http://www.predictiveservices.nifc.gov/intelligence/2016_Statsumm/intro_summary16.pdf. [Date accessed: May 30, 2017].
- National Interagency Coordination Center. 2018. Wildland fire summary and statistics annual report: 2017. https://www.predictiveservices.nifc.gov/intelligence/2017_statsumm/intro_summary17.pdf. [Date accessed: April 30, 2018].
- Nowacki, G.J.; Abrams, M.D. 2008. The demise of fire and “mesophication” of forests in the Eastern United States. *BioScience*. 58(2): 123–138.
- Nowacki, G.; Brock, T. 1995. Ecoregions and subregions of Alaska [EcoMap]. Version 2.0. Juneau, AK: U.S. Department of Agriculture Forest Service, Alaska Region. Map; presentation scale 1:5,000,000; colored.
- Potter, K.M. 2012a. Large-scale patterns of forest fire occurrence in the conterminous United States and Alaska, 2005–07. In: Potter, K.M.; Conkling, B.L., eds. Forest Health Monitoring 2008 national technical report. Gen. Tech. Rep. SRS-158. Asheville, NC: U.S. Department of Agriculture Forest Service, Southern Research Station: 73–83.

- Potter, K.M. 2012b. Large-scale patterns of forest fire occurrence in the conterminous United States and Alaska, 2001–08. In: Potter, K.M.; Conkling, B.L., eds. Forest Health Monitoring 2009 national technical report. Gen. Tech. Rep. SRS-167. Asheville, NC: U.S. Department of Agriculture Forest Service, Southern Research Station: 151–161.
- Potter, K.M. 2013a. Large-scale patterns of forest fire occurrence in the conterminous United States and Alaska, 2009. In: Potter, K.M.; Conkling, B.L., eds. Forest Health Monitoring: national status, trends and analysis, 2010. Gen. Tech. Rep. SRS-176. Asheville, NC: U.S. Department of Agriculture Forest Service, Southern Research Station: 31–39.
- Potter, K.M. 2013b. Large-scale patterns of forest fire occurrence in the conterminous United States and Alaska, 2010. In: Potter, K.M.; Conkling, B.L., eds. Forest Health Monitoring: national status, trends and analysis, 2011. Gen. Tech. Rep. SRS-185. Asheville, NC: U.S. Department of Agriculture Forest Service, Southern Research Station: 29–40.
- Potter, K.M. 2014. Large-scale patterns of forest fire occurrence in the conterminous United States and Alaska, 2011. In: Potter, K.M.; Conkling, B.L., eds. Forest Health Monitoring: national status, trends and analysis, 2012. Gen. Tech. Rep. SRS-198. Asheville, NC: U.S. Department of Agriculture Forest Service, Southern Research Station: 35–48.
- Potter, K.M. 2015a. Large-scale patterns of forest fire occurrence in the conterminous United States and Alaska, 2012. In: Potter, K.M.; Conkling, B.L., eds. Forest Health Monitoring: national status, trends, and analysis 2013. Gen. Tech. Rep. SRS-207. Asheville, NC: U.S. Department of Agriculture Forest Service, Southern Research Station: 37–53.
- Potter, K.M. 2015b. Large-scale patterns of forest fire occurrence in the conterminous United States and Alaska, 2013. In: Potter, K.M.; Conkling, B.L., eds. Forest Health Monitoring: national status, trends, and analysis 2014. Gen. Tech. Rep. SRS-209. Asheville, NC: U.S. Department of Agriculture Forest Service, Southern Research Station: 39–55.
- Potter, K.M. 2016. Large-scale patterns of forest fire occurrence in the conterminous United States, Alaska, and Hawaii, 2014. In: Potter, K.M.; Conkling, B.L., eds. Forest Health Monitoring: national status, trends, and analysis 2015. Gen. Tech. Rep. SRS-213. Asheville, NC: U.S. Department of Agriculture Forest Service, Southern Research Station: 41–60.
- Potter, K.M. 2017. Large-scale patterns of forest fire occurrence in the conterminous United States, Alaska, and Hawaii, 2015. In: Potter, K.M.; Conkling, B.L., eds. Forest Health Monitoring: national status, trends, and analysis 2016. Gen. Tech. Rep. SRS-222. Asheville, NC: U.S. Department of Agriculture Forest Service, Southern Research Station: 43–62.
- Potter, K.M. 2018. Large-scale patterns of forest fire occurrence in the conterminous United States, Alaska, and Hawaii, 2016. In: Potter, K.M.; Conkling, B.L., eds. Forest Health Monitoring: national status, trends, and analysis 2017. Gen. Tech. Rep. SRS-233. Asheville, NC: U.S. Department of Agriculture Forest Service, Southern Research Station: 45–64.
- Potter, K.M.; Koch, F.H.; Oswalt, C.M.; Iannone, B.V. 2016. Data, data everywhere: detecting spatial patterns in fine-scale ecological information collected across a continent. *Landscape Ecology*. 31: 67–84.
- Pyne, S.J. 2010. America's fires: a historical context for policy and practice. Durham, NC: Forest History Society. 91 p.
- Reams, G.A.; Smith, W.D.; Hansen, M.H. [and others]. 2005. The Forest Inventory and Analysis sampling frame. In: Bechtold, W.A.; Patterson, P.L., eds. The enhanced Forest Inventory and Analysis program—national sampling design and estimation procedures. Asheville, NC: U.S. Department of Agriculture Forest Service, Southern Research Station: 11–26.
- Richardson, L.A.; Champ, P.A.; Loomis, J.B. 2012. The hidden cost of wildfires: economic valuation of health effects of wildfire smoke exposure in southern California. *Journal of Forest Economics*. 18(1): 14–35.
- Schmidt, K.M.; Menakis, J.P.; Hardy, C.C. [and others]. 2002. Development of coarse-scale spatial data for wildland fire and fuel management. Gen. Tech. Rep. RMRS-87. Fort Collins, CO: U.S. Department of Agriculture Forest Service, Rocky Mountain Research Station. 41 p.

- Shima, T.; Sugimoto S.; Okutomi, M. 2010. Comparison of image alignment on hexagonal and square lattices. 2010 IEEE International Conference on Image Processing: 141–144. DOI: 10.1109/icip.2010.5654351.
- Tonini, M.; Tuia, D.; Ratle, F. 2009. Detection of clusters using space-time scan statistics. *International Journal of Wildland Fire*. 18(7): 830–836.
- U.S. Department of Agriculture (USDA) Forest Service. 2008. National forest type data development. http://svinetfc4.fs.fed.us/rastergateway/forest_type/. [Date accessed: May 13, 2008].
- U.S. Department of Agriculture (USDA) Forest Service. 2018. MODIS active fire mapping program: fire detection GIS data. <https://fsapps.nwgc.gov/afm/gisdata.php>. [Date accessed: January 12, 2018].
- Vinton, J.V., ed. 2004. *Wildfires: issues and consequences*. Hauppauge, NY: Nova Science Publishers, Inc. 127 p.
- White, D.; Kimerling, A.J.; Overton, W.S. 1992. Cartographic and geometric components of a global sampling design for environmental monitoring. *Cartography and Geographic Information Systems*. 19(1): 5–22.